Synthesis of Flagellin 22 As a Probe for Plant Signaling and Molecular Trafficking Towards Improved Crops

---

A thesis

presented to

the faculty of the Department of Chemistry

East Tennessee State University

In partial fulfillment

of the requirements for the degree

Master of Science in Chemistry

---

by

Edward Offei

December 2021

Dr. Robert F. Standaert, Chair

Dr. Gregory W. Bishop

Dr. Dane W. Scott

Keywords: plant signaling, Flagellin 22, molecular trafficking, solid-phase peptide synthesis

ABSTRACT

Synthesis of Flagellin 22 As a Probe for Plant Signaling and Molecular Trafficking Towards Improved Crops

by

Edward Offei

Plant signaling involves the transport of information within and between plant cells from receptors to effectors. It is known that many plant signaling molecules have profound effects on plants, through mechanisms that remain largely obscure. A key gap in knowledge is the understanding of the mechanisms that govern the movement of signaling molecules. This study seeks to synthesize signaling probes based on flagellin 22 (flg22), a 22-amino acid peptide that induces defense gene expression to trigger both local and systemic immune responses in plants. Solid-phase synthesis of fluorescently-tagged derivatives of flg22 was initiated, and studies on the uptake of labeled probes was conducted using a fiber-optic fluorescence microscope that was adapted for use in plants. Fluorescence microscopy showed uptake and internalization of TAMRA-flg22 in cells of *Arabidopsis thaliana* Columbia (wild-type strain), which was not observed in the *fls2* strain in which FLS2, the receptor for flg22, had been knocked out.

DEDICATION

This work is dedicated to my family and loved ones.

ACKNOWLEDGEMENTS

I would like to express my sincerest gratitude to Dr. Robert Standaert, my research advisor for the opportunity to be a part of his research group and also for his guidance and patience throughout this journey.

I would like to thank Dr. Gregory Bishop and Dr. Dane Scott for accepting to be a part of my advisory committee and for their help on my thesis.

I would like to thank Dr. Reza Mohseni for his help with instrumentation and analysis for my research work.

I am grateful to Ms. Maria Kalis for her help in administrative and organizational aspects throughout my time in graduate school.

I would also like to thank Dr. Jean Greenberg, Dr. Joana Jelenska and Ms. Jessica Morgan of the University of Chicago, Dr. Jennifer Morrell-Falvey of Oak Ridge National Laboratory and my research colleagues, Thomas Ntim, Christopher Erb, Opeyemi Tade, Enoch Asimbisa and John Hayford Teye-Kau for their help and support during the entire project. Special thanks go to Thomas and Christopher for their collaboration on the plant experiments and development of the microscope.

I would also like to thank Dr. Aruna Kilaru and Mr. Jyoti Behera for their help and assistance in growing our plants.

Special gratitude is owed to the United States Department of Energy for funding this research.

TABLE OF CONTENTS

LIST OF FIGURES

LIST OF ABBREVIATIONS

Boc	*tert*-Butoxycarbonyl
But	*tert*-Butyl
DBF	Dibenzofulvene
DCC	Dicyclohexylcarbodiimide
DCM	Dichloromethane
DIC	Diisopropylcarbodiimide
DIPEA	*N*,*N*-Diisopropylethylamine
DMF	*N*,*N*-Dimethylformamide
DTE	Dithioerythritol
E1CB	Elimination unimolecular conjugate base
EDT	1,2-Ethanedithiol
Flg22	Flagellin 22
FLS2	Flagellin sensitive 2
FLS3	Flavonol synthase 3
Fmoc	9-Fluorenylmethoxycarbonyl
FOV	Field of View
HATU	1-[Bis(dimethylamino)methylene]-1H-1,2,3-triazolo[4,5-b]pyridinium 3-oxid hexafluorophosphate
HBTU	*N*,*N*,*N*′,*N*′-Tetramethyl-*O*-(1*H*-benzotriazol-1-yl)uronium hexafluorophosphate, *O*-(Benzotriazol-1-yl)-*N*,*N*,*N*′,*N*′-tetramethyluronium hexafluorophosphate
HOBt	1-Hydroxybenzotriazole
LED	Light emitting diode
MAP	Mitogen activated protein
MAMPs	Microbe-associated molecular patterns
NMP	*N*-Methylpyrrolidinone
Pbf	2,2,4,6,7-Pentamethyldihydrobenzofuran-5-sulfonyl

PyBOP	Benzotriazol-1-yl-*N*-oxy-tris(pyrrolidino)phosphonium hexafluorophosphate
ROS	Reactive oxygen species
SPPS	Solid-phase peptide synthesis
TAMRA	5-Carboxytetramethylrhodamine
TFA	Trifluoroacetic acid
TLR5	Toll-like receptor 5
Trt	Triphenylmethyl (trityl)

CHAPTER 1. INTRODUCTION

Plant Signaling

Plants are sessile in nature, so they must have the ability to perceive, anticipate and respond to environmental changes to maximize their ability to survive and reproduce. Plants use signaling networks to coordinate their growth, development and responses to the environment. If fluctuations in conditions (e.g., changes in temperature, water availability, salinity, or nutrients) occur during key growth phases, plants sense these fluctuations and integrate the information to alter signaling outputs.[1] These conditions lead to the production of a number of toxic compounds, such as reactive oxygen species (ROS), including hydrogen peroxide, hydroxyl radical and superoxide, which have harmful effects on the physiology of plants. Plant signaling defines how plant cells respond to their environment and the transport of information within and between plant cells from receptor systems to effectors.[2] Plants' adaptation to abiotic stress (see Figure 1) is often dependent on stimulation of series of biochemical steps involving stress perception, signal transduction and the expression or repression of particular stress-related genes and metabolites.[3] Collectively these events constitute signal transduction pathways. They amplify and spread the original signal, often throughout the whole plant.[4]

Figure 1. Biotic and abiotic stress conditions

In order to provide a good crop yield and avoid premature senescence, plants must have defense mechanisms to combat the effect of these stress conditions. Plants sense external stress from their environment and generate an appropriate defensive response when attacked by a pathogen. The generation of the appropriate cellular responses operates by relaying stimuli from sensory receptors on the surface of the cell. When signal molecules bind, the receptor undergoes a conformational change that propagates across the cell membrane (transduction) to the cytoplasm. There, a signal cascade results that leads to altered gene expression in the nucleus of the cell, creating a multifaceted response which results in tolerance against a stress condition by plants.[5]

Signaling pathways can involve a wide variety of biochemical events, such as changes in intracellular Ca^{2+} levels,[6] rapid phosphorylation and dephosphorylation of proteins,[7] and activation of G-proteins, that amplify the signal and result in multiple effects.

Flagellin 22

This study focuses on the plant signaling molecule flagellin 22 (flg22). Flg22, a 22 amino acid peptide with its amino acid sequence derived from the N-terminus of the flagellin protein of the flagellum in most Gram-positive bacteria (see Figure 2). Specifically, I sought to study how flg22 enters and is trafficked in plants. Flg22 is in a class of molecules known as microbe-associated molecular patterns (MAMPs). It is known to elicit specific innate immune responses in both plant and animals.[8,9] Flagellin, or the fragment flg22, is a signal to plants that a bacterium is present. It is perceived by the receptor flagellin sensitive 2 (FLS2), which is homologous to the mammalian toll-like receptor 5 (TLR5), a leucine-rich repeat-containing receptor-like kinase.[10]

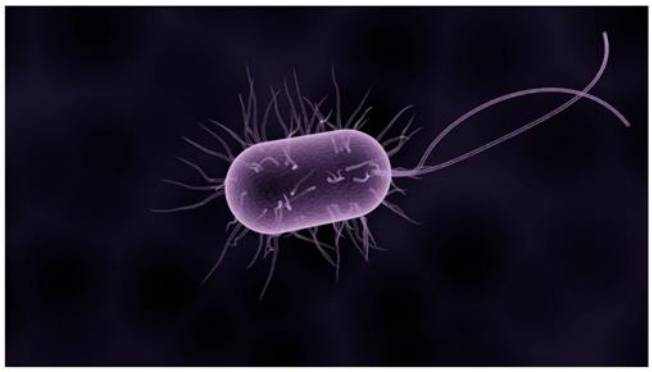

Figure 2. Structure of a flagellated bacterium. Flagella are the long fibers at right. Image source: public domain image from Reference 56.

Recognition of flg22 by FLS2 leads to several events, notably activation of a MAP kinase phosphorylation cascade, resulting in activation of transcription factors and expression of defense genes in the nucleus. ROS are produced locally, and a long-range effect also results, conveying to plants the ability to protect themselves against fungal and bacterial infections.[11] In the process, FLS2 is internalized into the cell by endocytosis.[12] A study by Jelenska and

coworkers showed that flg22 itself can migrate throughout plants, and that that long-distance trafficking was via FLS2.[13]

Plants belonging to the Solanaceae family such as pepper, tomato and potato recognize bacterial flagellin by the FLS3 receptor. The FLS3 receptor recognizes flgII-28, which is a 28-residue peptide from the internal region of bacterial flagellin, not the N-terminal region like flg22. While the region recognized by the FLS3 receptor is different, it similarly protects leaf tissues against bacterial infection through the enhancement of immune responses.[14]

The study of flagellin and its receptors in plants is aided by plant genetic techniques. For example, plants mutated to knock out the *fls2* gene exhibit weakened or damaged ability in binding to flg22,[15] while plants having their FLS2 receptor tagged with green fluorescent protein (GFP) allow observation of molecular trafficking by fluorescence microscopy.[13] As these examples illustrate, genetics and microscopy are a powerful combination for studying molecular trafficking in plants. My research seeks to synthesize flg22 with a fluorescent dye using solid-phase peptide synthesis, and to use the fluorescent probe in development of a novel fiber-optic microscope for studying flg22 and FLS2 in plants. The advantage of the fiber-optic microscope is that it can be used on live plants for non-destructive, long-term studies.

Solid Phase Peptide Synthesis (SPPS)

Peptides play a pivotal role in biological, medical and pharmaceutical research. For over a century, the synthesis of polyamide molecules has been a major focus in the field of organic chemistry. In 1903, the first successful coupling of two amino acids by Emil Fischer was performed via acyl chlorides. There was no suitable amino-protecting group at this time available for synthesizing longer peptides.[16] The method conceived by R.B. Merrifield, assembling

peptides anchored on a solid support, was a breakthrough and great achievement which had enormous impact on the further development of peptide synthesis, and for which Merrifield was awarded the Nobel Prize in Chemistry in 1984. Solid phase peptide synthesis offers multiple advantages over synthesis in solution, in that purification or isolation of intermediates is not required, the insolubility of oligopeptides is overcome, and rapid assessment of reaction completion by simple color assay (Kaiser test) is available.[17] Another advantage of SPSS is that it allows use of excess monomer at high concentration to drive coupling reactions to completion quickly, with excess reagent and byproducts removed at the end of the reaction by simple washing operations.[18] The application of SPPS at the very beginning of its implementation required use of liquid hydrogen fluoride and had other limitations. Therefore, milder chemistries and appropriate SPPS solid supports had to be developed, and advanced methods introduced to prevent undesired side-reactions.[19]

In recent years, the approach to peptide synthesis has yielded impressive successes in the synthesis of biologically active peptides such as systemins and phytosulfokine.[20] The development and availability of new techniques and reagents puts the synthesis of most small peptides in easy reach. However, the synthesis of long chain polypeptides with these synthetic methods is not typically feasible due to technical difficulties encountered with solubility and purification. These difficulties become very significant as the number of the amino acid residues being coupled increases.[21]

SPSS is performed in the C→N direction, the opposite of protein synthesis *in vivo*. That is, assembly of the peptide chain begins at the carboxy or C-terminal residue, which is attached to the solid-phase resin via its carboxyl group. The complete chain is constructed by the successive addition of protected amino acids to the N-terminus of the immobilized chain (Figure

3).[22] As the growing chain is bound to a solid support, excess reagents and byproducts are removed by simple filtration after each coupling and deprotection step. Washing with an appropriate solvent such as *N*-methyl-2-pyrrolidinone (NMP) or *N*,*N*-dimethylformamide (DMF) ensures complete removal and allows for rapid iteration.[23] After all amino acid monomers have been added, any remaining protecting groups are removed, and the peptide is cleaved from the resin.

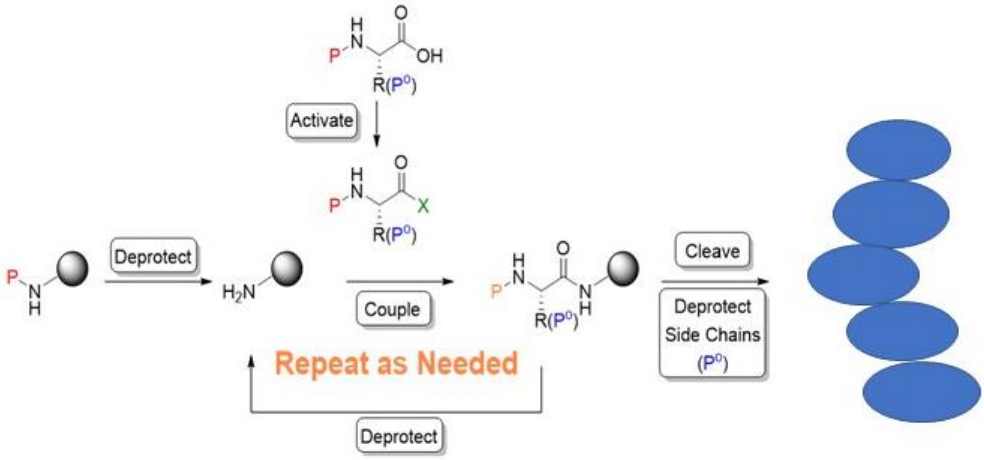

Figure 3. General process of solid-phase peptide synthesis. P° indicates orthogonal protection on the amino acid side chain. Blue ovals represent amino acid units in the completed peptide.

The initial stage of SPPS is the swelling of the resin, which is typically cross-linked polystyrene, usually with NMP or DMF.[24] Swelling is very important because the reaction kinetics are diffusion-controlled. The more the resin swells, the higher the rate of diffusion of the reagents into the core of its matrix.[25] Full swelling allows shorter reaction times and more complete chemical conversion. After swelling, each bead is essentially a microreactor. Size-

selected beads are used, as significant differences in the sizes of the beads can result in impure products due to inconsistent chemistry.

The next step after swelling is selective deprotection or liberation of the N-terminal amino group from its protecting group so it can form a peptide bond without affecting the side chain protecting groups. Protecting groups for the backbone and side-chain functional groups are of critical importance. The ability to remove one protecting group without affecting the others is a very important feature of the synthesis. Protecting groups that can be removed in the presence of the other, in any order, without affecting the other, are called orthogonal.[26] Thus, if a base-labile protecting group is used on the backbone α-amino groups, side chains are protected with orthogonal acid-labile groups that are stable to base and will survive multiple operations of selective deprotection and coupling as the desired chain has been assembled (Figure 4).

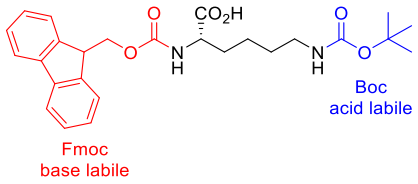

Figure 4. Structure of the amino acid lysine bearing the orthogonal Fmoc and Boc protecting groups

The most preferred protecting groups for the α-amino group are urethanes, ROCO–, the most popular being benzyloxycarbonyl (Cbz or Z), *tert*-butoxycarbonyl (Boc), and 9-fluorenylmethoxycarbonyl (Fmoc). The different alkyl substituents provide orthogonal reactivity. Boc is susceptible to acid, Fmoc to base, and Cbz to catalytic hydrogenolysis, Birch reduction, and certain nucleophiles. Simple acyl groups like acetyl are as stable as the peptide

linkages and cannot be removed without destroying the peptide itself. Urethanes also provide superior resistance to racemization during coupling.

Cleavage of the Backbone Protecting Group

The most widely used strategy in solid phase peptide synthesis for the forty years since its inception and implementation is the Fmoc strategy,[27] which uses Fmoc for protection of the backbone α-amino groups and acid-labile groups such as Boc for the protection of side chains. A large pool of different protecting groups is used for the various amino acid side chains. Reagents and strategies for different steps used in this route have been constantly developed and improved over the years.[28] The removal of the Fmoc group in SPPS as illustrated in Figure 5 proceeds via an E1CB reaction mechanism, which is a two-step mechanism. The first is removal of the acidic proton at the 9-position of the fluorene ring system by a mild base, preferably a secondary amine like piperidine, and the second is a β-elimination that yields a reactive dibenzofulvene (DBF) byproduct. The unusually high carbon-acidity of the proton at the 9-position is a result of the aromaticity of the conjugate base. Reactions of this sort work better in an relatively polar solvent (DMF or *N*-methylpyrrolidinone [NMP]) compared to dichloromethane (DCM), which is a relatively non-polar one.[29] Disruption of interchain aggregation is less effective with DMF than with NMP.

The use of primary and tertiary amines for the removal of the Fmoc protecting group is also possible, but the most convenient and effective method employs the use of cyclic secondary amines because of their balance of basicity and nucleophilicity. They effectively and efficiently trap the reactive DBF byproduct to generate a stable adduct (Figure 5), thereby driving the deprotection of the Fmoc protecting group to completion.[30,31,32]

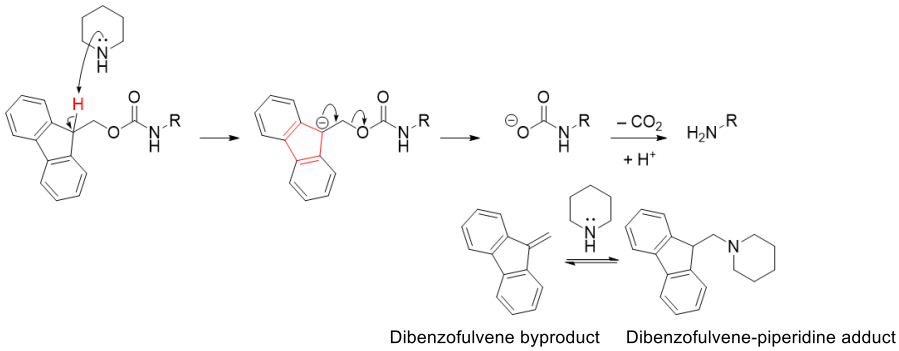

Figure 5. Fmoc deprotection via the E1CB mechanism

Kaiser Test

After cleavage of the protecting group, SPPS allows a color assay test to determine successful deprotection. This color assay is called the Kaiser test.[17] Very sensitive to primary amines, the Kaiser test is used to verify the completeness of deprotection and coupling reactions. Ninhydrin, one of the test reagents, reacts with the free N-terminal amino group of the growing peptide chain to produce an intense blue or purple color (Ruhemann's purple), indicating complete deprotection, as shown in Figure 6. For the detection of secondary amines, the Kaiser test is not efficient or reliable. For amino acids with secondary N-termini, such as proline or pipecolic acid, another test such as the isatin test or the chloranil test is used.[17]

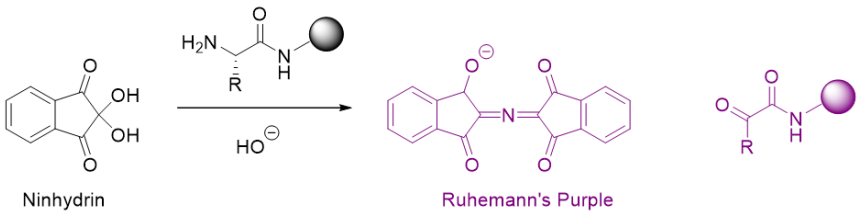

Figure 6. Reaction of ninhydrin with a free N-terminal amino group

Peptide Coupling

Once deprotection is complete, the next step is to couple or attach the next amino acid to the growing peptide chain. The coupling stage is commonly understood to be the most significant and demanding reaction in SPSS. Poor couplings result in low yields, create deletions and allow side reactions such as racemization, making purification more difficult and time-consuming. Before it can react with the amino terminus of the growing chain, the carboxyl group of the amino acid to be attached must be activated using coupling reagents or activators for rapid and quantitative amide bond formation. One of the most popular and simplest carboxyl activation reagents first used by Merrifield was dicyclohexylcarbodiimide (DCC).[33] The reaction is performed in DCM or DMF. The use of DCC liberates dicyclohexylurea as a byproduct, which is poorly soluble in most organic solvents.[34] This feature makes DCC very efficient in solution-phase reactions but less well suited for solid-phase reactions. Moreover, partial racemization occurs with the use of DCC to activate the carboxyl group because the *O*-acylisourea intermediate is highly reactive.

The introduction of 1-hydroxybenzotriazole (HOBt, Figure 7) as an additive greatly reduces racemization because it leads to the formation of a more stable benzotriazolyl ester.[35] This active ester is intermediate in reactivity between an ordinary ester and a carboxylic anhydride or *O*-acylisourea. It reacts rapidly with amines but slowly with water and alcohols, and it racemizes slowly. HOBt is used in excess to trap the *O*-acylisourea quickly before appreciable loss of configuration. Another advance was the development of phosphonium and uronium reagents for coupling, such as benzotriazol-1-yl-*N*-oxy-tris(pyrrolidino)phosphonium hexafluorophosphate (PyBOP)[36] and *N*-[(1H-Benzotriazol-1-yl)(dimethylamino)-methylene]-*N*-methylmethanaminium hexafluorophosphate *N*-oxide (HBTU)[37] (Figure 7). Coupling with these

salts must be performed with excess HOBt and a base, usually *N*,*N*-diisopropylethylamine (DIPEA).[38] The mechanism of the reaction with PyBOP, used in this study, is shown in Figure 8.

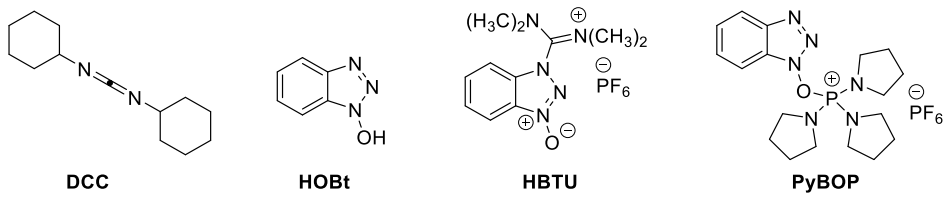

Figure 7. Examples of peptide coupling reagents

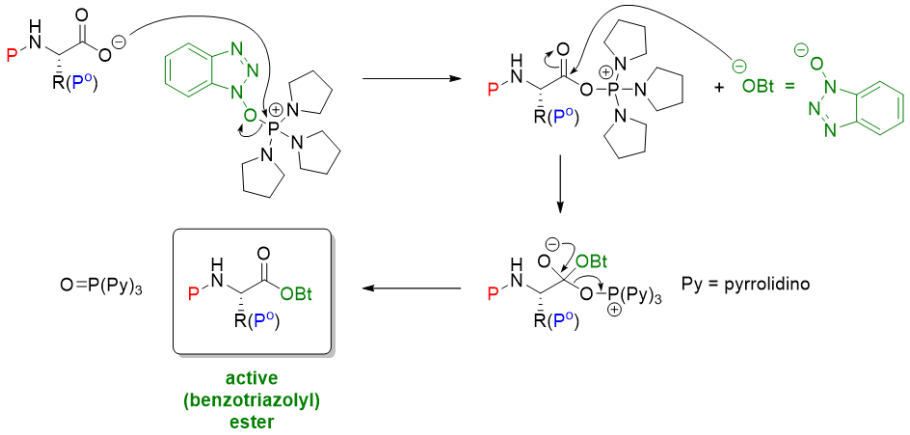

Figure 8. Reaction mechanism of PyBOP coupling

After the desired sequence has been assembled, the synthesized peptide needs to be cleaved off the resin and concomitantly freed of all side-chain protecting groups. The standard reagent used in performing this final cleavage of the peptide from the resin is TFA. Highly reactive carbocations are generated during this reaction that have to be trapped to avoid the formation of any undesired product by reaction with amino acids such as cysteine, threonine, serine, and tyrosine, all of which are very reactive toward electrophiles.

Other reagents called scavengers are added for this reason. The advantages of different scavenger cocktails have been analyzed in the several reports.[39] Water is a moderately efficient scavenger that can be added at ~2.5% (v/v) for the cleavage of peptides that are without cysteine and tryptophan in their amino acid sequence. Trialkylsilanes are efficient cation scavengers and are typically added at a similar concentrations.[40] For peptides containing sensitive amino acids, 1,2-ethanedithiol (EDT) and dithioerythritol (DTE) are the most efficient and often used scavengers.

After successfully synthesizing flg22, this peptide will be delivered into our model plant, *Arabidopsis thaliana.*

Arabidopsis thaliana

Arabidopsis thaliana, a flowering plant has over the years become the plant of choice for a wide range of studies in plant sciences.[41] *Arabidopsis* can be grown in petri plates or maintained in pots located either in a greenhouse or under fluorescent lights in a growth chamber in the laboratory, and it produces seeds in abundance.[42]

The ability of *Arabidopsis* to be genetically modified easily is a significant advantage and a major reason why it is the most-used model plant and why it was chosen as the model plant for this study. For molecular and genetic studies, Colombia and Landsberg are standard ecotypes used as wild-type plants for experimental analysis. The entire life or growth cycle of the plant, which comprises seed germination to when first seeds are produced, takes 6 weeks.[43] *Arabidopsis* is small, with rosettes that can grow from 2 to 10 cm in diameter and flowers about 2 mm long. As buds open, *Arabidopsis* self-pollinates. It can also be cross pollinated by the application of pollen to the surface of the stigma.

The small size of the *Arabidopsis* genome and the small number of chromosomes (5–8) makes it very amenable to genetic mapping and sequencing.[44] The ability of *Arabidopsis* to self-pollinate is an important feature that facilitates genetic experiments. *Arabidopsis* can be transformed using *Agrobacteria* by dipping the flowers into a culture of the bacteria containing a suitable vector.[45] There is an extensive set of resources developed through research using *Arabidopsis*. These resources include vast collections of mutants with different phenotypes, procedures for performing mutagenesis and genetic crosses, and methods for introducing exogenous DNA through transformation.[45] Thousands of mutants of *Arabidopsis* that are defective in almost every aspect of plant growth and development have been created.[46] These mutant plants have led to the elucidation of pathways responsible for development of leaves and roots, senescence, flowering, signal transduction, hormonal responses and many other cellular physiological processes.[47]

Another area where *Arabidopsis* have been used as a model plant is in the study of flower development. Studies in *Arabidopsis* are generally applicable to other flowering plants. The basic organs involved in the development of a flower are the sepals, carpels, petals and stamens. The arrangement of these flower-developing organs is in a series of whorls from the outside to the inside of the plant. The transformation of one of these organs to another can occur in *Arabidopsis*. A typical example is agamous mutation, where the stamens are transformed into petals with the replacement of the carpels by a new flower.[48] The result of this pattern is a sepal-petal-petal pattern.

Coen and Meyerowitz formulated a model known as the ABC model for flower development.[49,50] This model was based on the observation of the transformation of one organ to another arising from mutations. The floral organ identity genes of flowering plants according to

this model are grouped into three classes, namely Class A genes, which affect the petals and sepals; Class B genes, which affect the stamens and petals; and Class C genes, which affect carpels and stamens.

Research Aims

Flg22 has been widely used in plant defense studies. Its receptor, FLS2, has also been discovered and found to be internalized by endocytosis in epidermal cells after binding flg22.[12] Long-distance trafficking of flg22 has also been observed using a radiolabeled probe.[13] The goal of this research is to discern the underlying basis of the flg22 signaling network by synthesizing flg22-based fluorescent probes that can be delivered into our model plant *Arabidopsis* and tracked *in vivo* plants using a fiber-optic fluorescence microscope. The advantage of this approach over previous ones is that it enables long-term studies in live plants, with repeated observations. Use of confocal fluorescence microcopy typically requires excision of plant tissue. Radiochemical imaging is highly sensitive but cannot provide subcellular resolution, and imaging methods such as autoradiography are also destructive to the plant.

The aims of this research were:

1. To synthesize fluorescently tagged flg22 probes; and
2. To track flg22 in live plants using fluorescence microscopy after developing the fiber optic microscopy platform to obtain high quality plant images.

CHAPTER 2. EXPERIMENTAL METHODS

Chemicals and Instruments

Alanine Wang resin (Fmoc-Ala-Wang resin, 0.64mmole/g), isoleucine (Fmoc-Ile-OH), glutamine (Fmoc-Gln(Trt)-OH), leucine (Fmoc-Leu-OH), glycine (Fmoc-Gly-OH), alanine (Fmoc-Ala-OH·H_2O), aspartic acid (Fmoc-Asp(But)-OH, lysine (Fmoc-Lys(Boc)-OH, serine (Fmoc-Ser(But)-OH), asparagine (Fmoc-Asn(Trt)-OH), arginine (Fmoc-Arg(Pbf)-OH), threonine (Fmoc-Thr(But)-OH), benzotriazol-1-yl-N-oxy-tris(pyrrolidino)phosphonium hexafluorophosphate (PyBOP) and *N*-methyl-2-pyrrolidinone (NMP) were purchased from Creosalus. *N*,*N*-Diisopropylethylamine (DIPEA, 99.5+%) and pyridine (99+%) were obtained from Acros Organics. Piperidine (99%) and phenol (99%) were purchased from Alfa Aesar. Trifluoroacetic acid (TFA), hydrochloric acid (HCl), dichloromethane (DCM) and potassium cyanide were all purchased from Fisher Scientific. Ninhydrin was obtained from Sigma. 1-Hydroxybenzotriazole (HOBt hydrate) was purchased from Oakwood Chemical, and triisopropylsilane was obtained from TCI America. The sample of TAMRA-flg22 used in plant imaging experiments was the generous gift of Ms. Jessica Morgan (University of Chicago).

Plants

Seeds of *Arabidopsis thaliana* Colombia and the transgenic line *fls2* were obtained from the greenhouse at the University of Chicago. Seeds were vernalized by keeping in 0.1% agar at 4°C for 4 d, after which they were planted in potting soil (Miracle-Gro® Potting Mix with Fertilizer, part number 74278300, mixed with 2 qt of perlite per 1 cf of potting mix) and kept in a Percival growth chamber at 22–24 °C with relative humidity of 60–70%, and illumination at 100–150 µmol $M^{-2}sec^{-1}$ illumination with a 16 hour light/8 hour dark cycle for 4 weeks.

Synthesis of Flg22 via Solid Phase Peptide Synthesis

A representative procedure is provided for flg22. Fmoc-Ala Wang resin (30 µmol, 50 mg) was swelled in 2 ml of NMP in a 2-mL plastic syringe with a pressed-in filter frit (Torviq). All steps (swelling, washing, coupling and deprotection) were performed with gentle rotation of the reaction vessel on a mini-rotator. After removal of the solvent, the N-terminal Fmoc group was deprotected with 20% piperidine in NMP for 30 minutes. The deprotected resin was washed six times with 2 mL of NMP for 2 min/wash to remove piperidine completely. A Kaiser test was performed to verify complete deprotection. For this purpose, about 10–15 beads of the resin, and 2 to 3 drops of the Kaiser test reagents,[17] were placed in a test tube and heated with a heat gun. A positive result was indicated by development of a dark blue or purple color on the beads.

In the first coupling, Fmoc-Ile-OH (32 mg, 90 µmol, 3.0 equiv) was dissolved in 200 µL of NMP, to which was added 56 µL of PyBOP (0.9 M in NMP, 50 µmol, 1.67 equiv), 50 µL of HOBt (1.0 M in NMP, 50 µmol, 1.67 equiv) and 18 µL (100 µmol, 3.3 equiv) of DIPEA. The resulting solution was added to the resin in the reaction vessel and rotated for 90 min to allow coupling to take place. After expulsion of the reaction mixture through the frit, the resin again was washed 6× with 2-mL portions of NMP to remove all unwanted products and reagents. Success of the coupling was verified by a negative Kaiser test. Subsequent cleavage of the Fmoc protecting group and washing were performed as described above, and success verified with a positive Kaiser test.

The above cycle was repeated for each subsequent amino acid to complete the flg22 sequence (H-Gln-Arg-Leu-Ser-Thr-Gly-Ser-Arg-Ile-Asn-Ser-Ala-Lys-Asp-Asp-Ala-Ala-Gly-Leu-Gln-Ile-Ala-OH) using the same stoichiometry and the following Fmoc-amino acid derivatives: Fmoc-Gln(Trt)-OH (55 mg), Fmoc-Leu-OH (32 mg), Fmoc-Gly-OH (27 mg), Fmoc-

Ala-OH·H_2O (30 mg), Fmoc-Ala-OH·H_2O (30 mg), Fmoc-Asp(But)-OH (37 mg), Fmoc-Asp(But)-OH (37 mg), Fmoc-Lys(Boc)-OH (42 mg), Fmoc-Ala-OH·H_2O (30 mg), Fmoc-Ser(But)-OH (35 mg), Fmoc-Gly-OH (27 mg), Fmoc-Thr(But)-OH (36 mg), Fmoc-Ser(But)-OH (35 mg), Fmoc-Leu-OH (32 mg), Fmoc-Arg(Pbf)-OH (58 mg) and Fmoc-Gln(Trt)-OH (55 mg).

After removal of the final Fmoc group, the resin was washed with NMP (6×), methanol (3×) and DCM (3×), then allowed to dry in the air. The peptide was deprotected and cleaved from the resin using 1 mL of a cleavage cocktail containing 950 µL of TFA, 25 µL of H_2O and 25 µL of triisopropylsilane. After a 30-min reaction time with agitation, the cocktail was withdrawn and the resin washed with an additional 1 mL of TFA. The combined TFA solutions were evaporated under nitrogen, and the crude peptide was obtained by washing the residue with ether.

In the same fashion, a scrambled version of flg22 was synthesized for use as a negative control. The scrambled peptide has identical amino acid composition but an arbitrary sequence: GITASKALGADLRRINQSASQD.

Fiber-Optic Epifluorescence Microscope

The basic fiber-optic fluorescence microscope was constructed by Dr. Robert F. Standaert using an adaptation of literature designs (Figure 9).[51,52] Images were obtained at 2.3× native magnification using a GRIN endoscopic objective lens (Grintech, GT-MO-080-032-ACR-VISNIR-08-00, 0.75 NA, 80-µm working distance in water) cemented to a 1-m coherent imaging fiber (Fujikura FIGH-30-850N, 30,000 fibers, 1 m length); use of the magnifying objective provides a field of view (FOV) 340 µm in diameter. Fluorescence excitation was provided by independent LED light sources centered at ~470 nm and ~565 nm for excitation of

fluorescein/GFP and tetramethylrhodamine chromophores, respectively. A dual-band filter/beamsplitter set (Chroma Technologies, set 59004) and a color camera (FLIR Technologies Grasshopper 3.0 equipped with a Sony IMX252 sensor) were used to allow independent or simultaneous observation of both channels without changing filters. The optics were configured as illustrated in Figure 9, and images were captured on a laptop computer using the camera manufacturer's SpinView or Spinnaker software. Except as indicated above, optical components were obtained from Thorlabs. Modifications to the sample stage were performed in collaboration with Mr. Thomas Ntim and Mr. Christopher Erb.

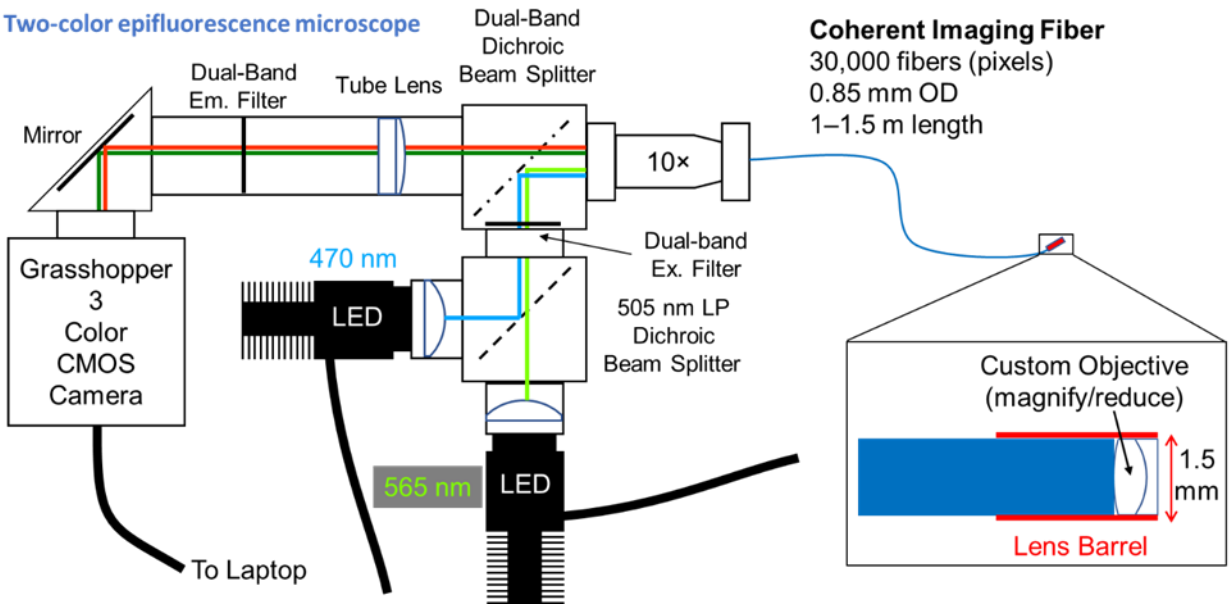

Figure 9. Custom built fiber optic fluorescence microscope. Image copyright Robert F. Standaert, used with permission.

Treatment of Plants with TAMRA-flg22 and Imaging

Leaves of *Arabidopsis* Colombia and the *fls2* transgenic line were floated (abaxial side down) on solutions of 1 µM and 0.5 µM TAMRA-labelled flg22 solution (in water) overnight at room temperature (Figure 10). Leaves were washed after treatment by gently shaking them in water for several minutes, and the abaxial side was imaged at a distance of 80 µm using the custom-built fiber optic fluorescence microscope under green light (565 nm) excitation (Figure 9). The absorption and emission maxima of TAMRA are 552 nm and 578 nm, respectively. For the experiments discussed below, leaves were placed on standard 25.4 mm × 76.2 mm glass microscope slides, and images were obtained using the 3rd-generation microscope configuration with the fiber mounted to a conventional microscope body (Figure 14) providing X–Y translation and Z fine focus. Image acquisition was performed in the dark to minimize stray light.

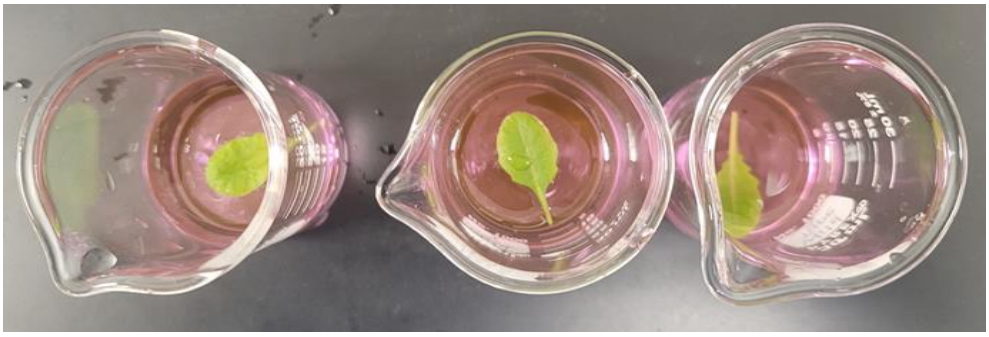

Figure 10. Delivery of TAMRA-flg22 to *Arabidopsis* leaves

CHAPTER 3. RESULTS AND DISCUSSION

Synthesis of Flg22

SPPS was preferred to solution-phase synthesis because the need to optimize reaction conditions and the purification procedures at every intermediate step render solution-phase synthesis labor intensive and time consuming. SPPS presented us with ability to synthesize peptides chains of up to 20 to 50 amino acids. The basic concept of the synthetic method used is to construct a polypeptide chain that has been anchored on an insoluble polymeric support (resin). SPPS allowed rapid assessment of reaction completion by the Kaiser test. This test was performed after every deprotection and coupling reaction. We observed the resin turn dark blue or purple (positive test) after every deprotection and remain colorless (negative test) after every coupling reaction. Beads turning dark blue or purple (Figure 11) indicated complete deprotection as a result of the formation of Ruhemann's purple from the reaction between ninhydrin and the free amino group of the growing peptide chain. The formation of colorless beads after coupling showed the absence of a free amino group, indicating complete reaction because the amino acid added to the growing peptide chain has its N-terminus protected and does not react with ninhydrin.

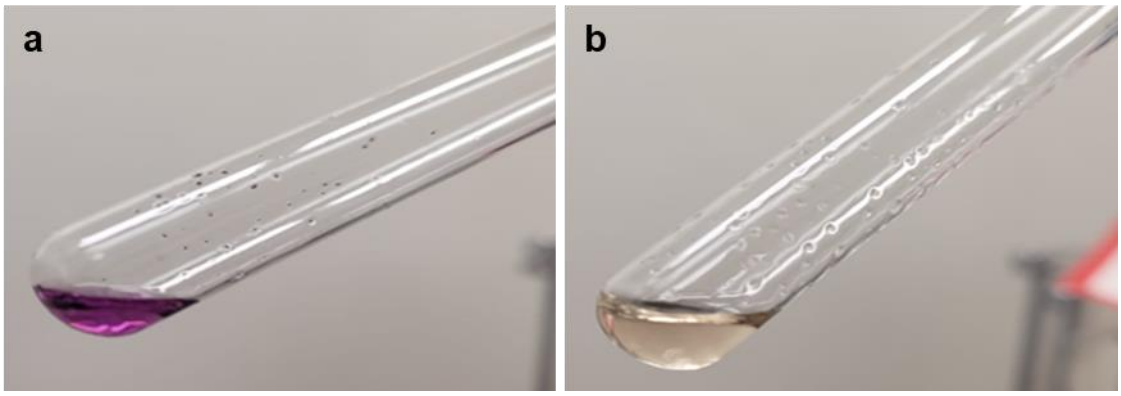

Figure 11. Kaiser test. a) Dark blue or purple beads on the wall of the test tube indicate complete deprotection (positive test). b) Colorless beads on the wall of the test tube indicate complete coupling (negative test).

All the amino acid derivatives used in the synthesis of flg22 had their N-terminal amino groups protected by Fmoc. The Fmoc group is base-labile and was removed with piperidine. Fmoc chemistry is more amenable to the laboratory setting than Boc chemistry, as it avoids the use of TFA for deprotection at each step, and liquid hydrogen fluoride for the final step. Hydrogen fluoride is extremely hazardous and requires the use of specialized apparatus.[53] The chemistry of Fmoc has now been well-enough developed that it is the primary method employed in the automated synthesis of polypeptides commercially.

Evaluation of Flg22 Uptake by Fiber-Optic Fluorescence Microscopy

To study the fate and movement of flg22 at the plant level, a fluorescently labelled version of flg22 was used. Specifically, the peptide was modified with an N-terminal 5-carboxytetramethylrhodamine (TAMRA) group so that it could be observed by fluorescence microscopy in plant tissues.

Positioning of the fiber optic probe and leaf sample proved to be a crucial in obtaining quality images. Development of the imaging platform proceeded through three stages and was

performed in collaboration with Mr. Thomas Ntim and Mr. Christopher Erb. At the outset of the project, only the optical part of the microscope had been completed. In this Gen 0 microscope, the probe had to be maneuvered by hand. Given that the working distance is 80 µm, and even a few µm of motion will unfocus the image, it was all but impossible to obtain plant images. The first attempt to mount the microscope's fiber optic probe utilized a ring stand, a plastic syringe barrel, and masking tape (Figure 12a). These component parts served to suspend the probe in such a way that specimens of *Arabidopsis* could be brought within focus of the probe and imaged 'by hand'. This primitive mounting adaptation proved difficult to operate, as it did not provide a means to securely fasten a plant specimen for controlled imaging and relied on the steadiness of one's hands alone to ensure image quality. Images obtained at this first mounting were usually very poor and out of focus (Figure 15b,c) making it impossible to discern any cellular uptake of flg22 in samples. Good images were occasionally obtained by chance.

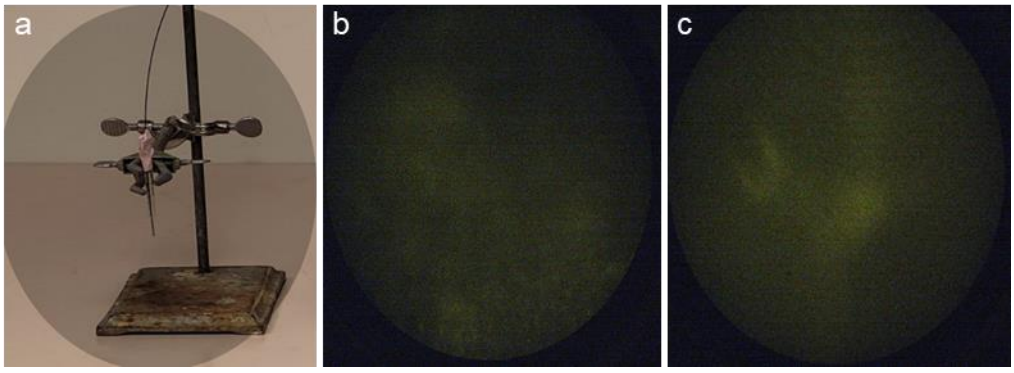

Figure 12. First-generation fiber-optic probe setup and imaging results. a) The fiber-optic probe clamped to a ring stand; b) and c) poor, out-of-focus images of Columbia and *fls2* leaves, respectively, after overnight incubation in 0.5 µM and 1µM TAMRA-flg22

The second-generation mounting implementation for the microscope's fiber optic probe utilized the same ring stand, plastic syringe, and masking tape but added a laboratory jack as a stage (Figure 13). Leaves were mounted on the stage in a petri dish. Steadiness of the hand in trying to image other areas of the leaf surface was again required, and images obtained were not much better than ones obtained from the first-generation mount.

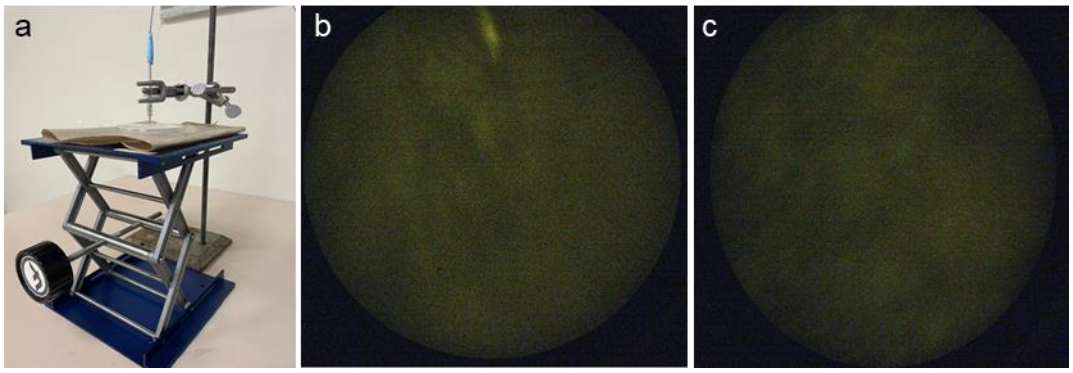

Figure 13. Second-generation fiber-optic probe setup and imaging results. a) The fiber optic probe clamped to a ring stand with a laboratory jack as a stage; b) and c) poor, out-of-focus images of Colombia and *fls2* leaves, respectively after overnight incubation in 0.5 µM and 1µM TAMRA-flg22.

The third fiber optic mounting generation (Figure 14) made use of cannibalized and repurposed parts from a conventional light microscope. By rearranging optics and assemblies from multiple, identical microscopes, a fixture was designed capable of safely immobilizing the fiber optic probe while maintaining the use of the stock light microscope stage (Figure 14). The stock stage allowed for 'X' and 'Y' translation of specimens on standard glass slides *in vitro*, and most importantly, for clear focus.

In this iteration, the fiber optic probe was secured inside a plastic pen barrel attached to the former optical lens portal of the light microscope. By carefully press-fitting the delicate fiber optic probe through the narrow orifice of the pen barrel, the risk of damaging the probe's

objective lens was significantly decreased. The risk of damaging the objective during imaging was a particular concern if the stage was raised to come in contact with the probe's lens (a likely scenario given the tolerance required of the imaging process). Press-fitting of the probe into the cylinder ensured that the probe could recede back into its plastic sheath if the stage applied too much pressure on the lens. This version of the imaging platform proved sufficient for evaluating cellular uptake of flg22. Images shown in Figures 15 and 16 were obtained with the third-generation fiber optic mounting.

Figure 14. Third-generation fiber-optic probe setup.

Using the third-generation microscope-based positioning system (Figure 14), the movement of TAMRA labelled flg22 was assessed after overnight treatment of the abaxial side of detached leaves of Columbia and *fls2 Arabidopsis* plants with 0.5 µM and 1 µM aqueous solutions of TAMRA-flg22. A water control was used, and little background fluorescence was noted in either plant strain (Figures 15a and 16a). The *fls2* line has the FLS2 receptor knocked out, so we did not expect localization of the labeled flg22 at the membrane or internalization. In

the experiment, treatment of an *fls2* leaf with 0.5 µM TAMRA-flg22 produced a result similar to water, with no clear probe fluorescence (Figure 15b). When 1 µM TAMRA-flg22 was used, there was pronounced uptake by stomata through an unknown but likely non-specific mechanism (Figure 15c). In addition, there was some diffuse fluorescence which might represent peptide on the surface of the leaf which had not been completely washed away. There was no clear intracellular fluorescence, but there was an unexpected observation of slight accumulation at the cell perimeters with the high concentration of TAMRA-flg22 (meandering lines circled in orange, Figure15c) of the *fls2* line. The binding could be non-specific, or might represent the presence of an unknown partner for flg22 in the membrane or cell wall that binds to peptide but does not lead to internalization. Further experiments are needed to follow up on this finding. An important negative control we were unable to perform is the use of scrambled flg22.

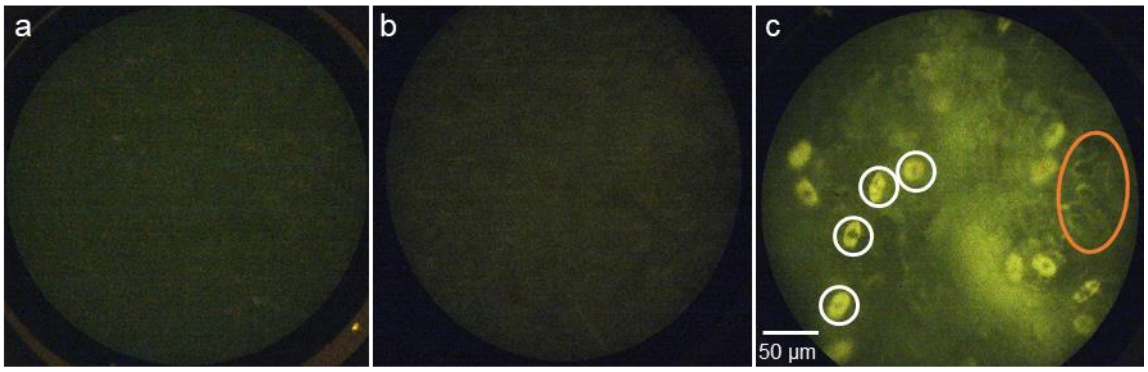

Figure 15. Transport of flg22 in *fls2*. (a) Control (b) Leaf treated with 0.5µM TAMRA-flg22 overnight, showing no uptake of probe by membranes or cells (c) Leaf treated with 1 µM TAMRA-flg22 overnight, showing uptake by the stomata (bright green spots circled in white) but not by epidermal cells (faint green meandering lines inside orange oval). Uptake of flg22 in the stomata is believed to be independent of the flg22 receptor, FLS2. Field of view (diameter of the image circle) is 340 µm.

Results with the Columbia plant provided a stark contrast. Even at the lower concentration of 0.5 µM TAMRA-flg22, there was pronounced localization of the probe at the cell perimeters (green meandering lines within the orange oval, Figure 16b), consistent with binding to the FLS2 receptor, as well as in stomata (bright green spots circled in white, Figure 16b). At 1 µM concentration, it appeared that some TAMRA-flg22 was taken up in the epidermal cells of Columbia (large area within the orange oval, Figure16c). Uptake in stomata was also observed, but it was receptor-independent, as it was observed in both Colombia and *fls2* lines. Uptake in epidermal cells of the plant should be specific, as we expect the peptide to be impermeant in the absence of the receptor.

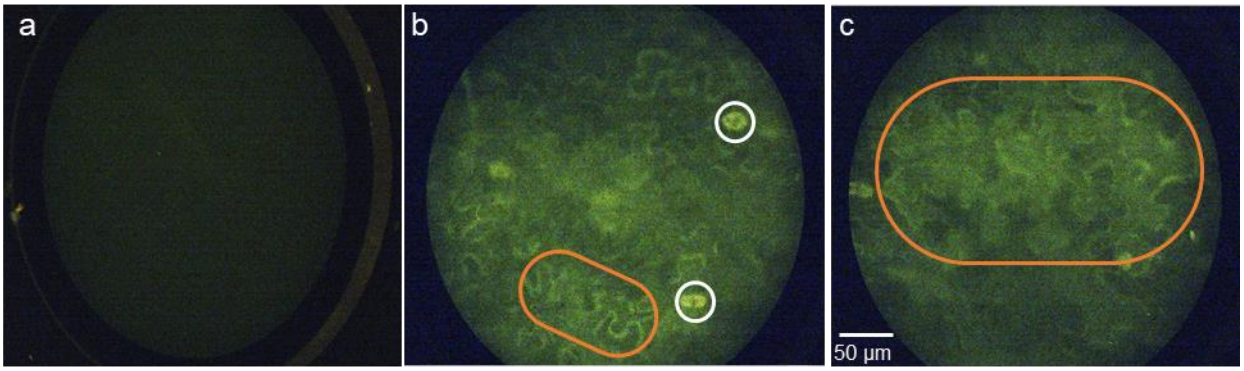

Figure 16. Transport of flg22 in Colombia. (a) Control (b) Leaf treated with 0.5µM TAMRA-flg22 overnight, showing uptake into guard cells of the stomata (bright green spots circled in white) and cell membranes (green meandering lines inside the orange oval) but not inside the cells (c) Leaf treated with 1 µM TAMRA-flg22 overnight, showing apparent uptake in cells after overnight incubation (inside the orange oval). Field of view (diameter of the image circle) is 340 µm.

Jelenska et al. conducted a similar experiment by delivering TAMRA labeled flg22 into Colombia and *fls2* plants. They observed transport of flg22 into the cells of Columbia, but none in the *fls2* line. Receptor-dependent uptake occurs in Columbia, thus there is strong signal in

Colombia but not in *fls2* plants. My study provided results consistent with the requirement of FLS2 for flg22 to show movement into cells via endocytosis.

The binding of flg22 to its receptor induces receptor endocytosis and initiates a cascade of signals to trigger local and systemic defense in plants.[54] We showed that flg22 accumulates at cell boundaries in Columbia plants containing the FLS2 receptor, but much less so in the *fls2* strain lacking the receptor. Further, we showed some apparent internalization of TAMRA-flg22, which presumably results from endocytosis. Assessment of long-range movement is a goal we were unable to realize within the time available. These findings are based on images obtained from the *fls2*, line where uptake was observed only in the guard cells of the stomata, which we hypothesize to be receptor independent. We hypothesize that the apparent internalization of flg22 is as a result of its receptor-mediated endocytosis.

CHAPTER 4. CONCLUSION AND FUTURE WORK

Flg22 and the innate immune response in plants are an important area of study, with implications for agriculture, bioenergy and human health. In this work, we sought to apply fluorescent probes of flg22 in conjunction with a fiber-optic fluorescence microscope for a better understanding of flg22 signaling. After proceeding through three generations of microscopy platforms to develop a workable setup for obtaining quality images at sub-cellular resolution, we were able to reproduce and verify key literature findings, as reported by Jelenska et al.[13] Specifically, we observed receptor-dependent localization of TAMRA-flg22 at cell periphery and apparent partial internalization of the peptide into pavement cells. Internalization is believed to occur through endocytosis of the flg22 receptor, FLS2. Consistent with this hypothesis, TAMRA-flg22 did not localize strongly to the membrane of *fls2* plants lacking the FLS2 receptor and did not enter the cells. An advance of the new microscopy platform is its suitability for non-destructive, repetitive, live-plant imaging, which has been a significant barrier in the field.

Labeled peptide used in this research was commercially synthesized. The flg22 core was re-synthesized to provide more material for future studies, as well as a starting point for the construction of additional probes. Limitations of time, equipment and materials prevented the final purification of the targeted probes by high-performance liquid chromatography, identification by mass spectrometry, and validation by *in-vivo* testing in *Arabidopsis* for biological effects and molecular trafficking. An unrealized goal is to use a different technique for delivery of peptides into the plant through the use of vertically aligned carbon nanofiber arrays.[55] This approach promises injury-free delivery of sub-microliter volumes of peptide solution into targeted tissues of model plants and will help fulfill the goal of performing peptide-trafficking studies in live plants.

We will also employ a fourth-generation fiber optic probe mount, which uses an AmScope 4-axis articulating arm, a precision X–Y–Z translation stage assembly with 3 mm travel in each dimension, a stainless steel pin vise, and ± 3° pitch and yaw control on the pin vise mount to enable *in vivo* imaging of specimens.

REFERENCES

(1) Mahajan, S.; Tuteja, N. Cold, Salinity and Drought Stresses: An Overview. *Arch. Biochem. Biophys.* **2005**, *444* (2), 139–158. https://doi.org/10.1016/j.abb.2005.10.018.

(2) Mulligan, R. M.; Chory, J.; Ecker, J. R. Signaling in Plants. *Proc. Natl. Acad. Sci. U. S. A.* **1997**, *94* (7), 2793–2795. https://doi.org/10.1073/pnas.94.7.2793.

(3) *Plant Signaling: Understanding the Molecular Crosstalk*; Hakeem, K. R.; Tahir, I.; Ul Rehman, R., Eds.; Springer, 2014. https://doi.org/10.1007/978-81-322-1542-4.

(4) Choi, W. G.; Toyota, M.; Kim, S. H.; Hilleary, R.; Gilroy, S. Salt Stress-Induced Ca^{2+} Waves Are Associated with Rapid, Long-Distance Root-to-Shoot Signaling in Plants. *Proc. Natl. Acad. Sci. U. S. A.* **2014**, *111* (17), 6497–6502. https://doi.org/10.1073/pnas.1319955111.

(5) Macrae, R. K.; Long, J. A. Transcriptional Regulation in Plants. *eLS* **2012**. https://doi.org/10.1002/9780470015902.a0023755.

(6) Poovaiah, B. W.; Reddy, A. S. N. Calcium and Signal Transduction in Plants. *CRC. Crit. Rev. Plant Sci.* **1993**, *12* (3), 185–211. https://doi.org/10.1080/07352689309701901.

(7) Felix, G.; Grosskopf, D. G.; Regenass, M.; Boller, T. Rapid Changes of Protein Phosphorylation Are Involved in Transduction of the Elicitor Signal in Plant Cells. *Proc. Natl. Acad. Sci. U. S. A.* **1991**, *88* (19), 8831–8834. https://doi.org/10.1073/pnas.88.19.8831.

(8) Newton, S. M. C.; Wasley, R. D.; Wilson, A.; Rosenberg, L.T.; Miller, J. F.; Stocker, B. A. Segment IV of a *Salmonella* Flagellin Gene Specifies Flagellar Antigen Epitopes. *Mol. Biol.* **1991**, *5(2)* (631), 419–425. https://doi.org/https://doi.org/10.1111/j.1365-2958.1991.tb02124.x.

(9) Ciacci-Woolwine, F.; Blomfield, I. C.; Richardson, S. H.; Mizel, S. B. *Salmonella*

Flagellin Induces Tumor Necrosis Factor Alpha in a Human Promonocytic Cell Line. *Infect. Immun.* **1998**, *66* (3), 1127–1134. https://doi.org/10.1128/iai.66.3.1127-1134.1998.

(10) Trdá, L.; Fernandez, O.; Boutrot, F.; Héloir, M. C.; Kelloniemi, J.; Daire, X.; Adrian, M.; Clément, C.; Zipfel, C.; Dorey, S.; Poinssot, B. The Grapevine Flagellin Receptor VvFLS2 Differentially Recognizes Flagellin-Derived Epitopes from the Endophytic Growth-Promoting Bacterium *Burkholderia Phytofirmans* and Plant Pathogenic Bacteria. *New Phytol.* **2014**, *201* (4), 1371–1384. https://doi.org/10.1111/nph.12592.

(11) Asai, T.; Tena, G.; Plotnikova, J.; Willmann, M. R.; Chiu, W. L.; Gomez-Gomez, L.; Boller, T.; Ausubel, F. M.; Sheen, J. MAP Kinase Signalling Cascade in *Arabidopsis* Innate Immunity. *Nature* **2002**, *415* (6875), 977–983. https://doi.org/10.1038/415977a.

(12) Robatzek, S.; Chinchilla, D.; Boller, T. Ligand-Induced Endocytosis of the Pattern Recognition Receptor FLS2 in Arabidopsis. *Genes Dev.* **2006**, *20* (5), 537–542. https://doi.org/10.1101/gad.366506.

(13) Jelenska, J.; Davern, S. M.; Standaert, R. F.; Mirzadeh, S.; Greenberg, J. T. Flagellin Peptide Flg22 Gains Access to Long-Distance Trafficking in *Arabidopsis* via Its Receptor, FLS2. *J. Exp. Bot.* **2017**, *68* (7), 1769–1783. https://doi.org/10.1093/jxb/erx060.

(14) Hind, S. R.; Strickler, S. R.; Boyle, P. C.; Dunham, D. M.; Bao, Z.; O'Doherty, I. M.; Baccile, J. A.; Hoki, J. S.; Viox, E. G.; Clarke, C. R.; Vinatzer, B. A.; Schroeder, F. C.; Martin, G. B. Tomato Receptor Flagellin-Sensing 3 Binds FlgII-28 and Activates the Plant Immune System. *Nat. Plants* **2016**, *2* (9), 1–8. https://doi.org/10.1038/nplants.2016.128.

(15) Chinchilla, D.; Bauer, Z.; Regenass, M.; Boller, T.; Felix, G. The *Arabidopsis* Receptor Kinase FLS2 Binds Flg22 and Determines the Specificity of Flagellin Perception. *Plant Cell* **2006**, *18* (2), 465–476. https://doi.org/10.1105/tpc.105.036574.

(16) Fischer, E.; Otto, E. Synthese von Derivaten Einiger Dipeptide. *Ber. Dtsch. Chem. Ges.* **1903**, *36* (2), 2106–2116. https://doi.org/10.1002/cber.190303602128.

(17) Kaiser, E.; Colescott, R. L.; Bossinger, C. D.; Cook, P. I. Color Test for Detection of Free Terminal Amino Groups in Solid Phase Peptide Synthesis. *Anal. Biachem*. **1970**, 34(2), 595–598. doi:10.1016/0003-2697(70)90146-6.

(18) Maurin, O.; Verdié, P.; Subra, G.; Lamaty, F.; Martinez, J.; Métro, T. X. Peptide Synthesis: Ball-Milling, in Solution, or on Solid Support, What Is the Best Strategy? *Beilstein J. Org. Chem.* **2017**, *13*, 2087–2093. https://doi.org/10.3762/bjoc.13.206.

(19) Coin, I.; Beyermann, M.; Bienert, M. Solid-Phase Peptide Synthesis: From Standard Procedures to the Synthesis of Difficult Sequences. *Nat. Protoc.* **2007**, *2* (12), 3247–3256. https://doi.org/10.1038/nprot.2007.454.

(20) Matsubayashi, Y.; Sakagami, Y. Peptide Hormones in Plants. *Annu. Rev. Plant Biol.* **2006**, *57*, 649–674. https://doi.org/10.1146/annurev.arplant.56.032604.144204.

(21) Bedford, J.; Hyde, C.; Johnson, T.; Jun, W.; Owen, D.; Quibell, M.; Sheppard, R. C. Amino Acid Structure and "Difficult Sequences" in Solid Phase Peptide Synthesis. *Int. J. Pept. Protein Res.* **1992**, *40* (3–4), 300–307. https://doi.org/10.1111/j.1399-3011.1992.tb00305.x.

(22) Amblard, M.; Fehrentz, J. A.; Martinez, J.; Subra, G. Methods and Protocols of Modern Solid Phase Peptide Synthesis. *Mol. Biotechnol.* **2006**, *33* (3), 239–254. https://doi.org/10.1385/MB:33:3:239.

(23) Stewart, J. M. Solid Phase Peptide Synthesis. *J. Macromol. Sci. Part A - Chem.* **1977**, *10* (1–2), 259–288. https://doi.org/10.1080/00222337608068099.

(24) Santini, R.; Griffith, M. C.; Qi, M. A Measure of Solvent Effects on Swelling of Resins

for Solid Phase Organic Synthesis. *Tetrahedron Lett.* **1998**, *39* (49), 8951–8954. https://doi.org/10.1016/S0040-4039(98)02069-3

(25) Pugh, K. C.; York, E. J.; Stewart, J. M. Effects of Resin Swelling and Substitution on Solid Phase Synthesis. *Int. J. Pept. Protein Res.* **1992**, *40* (3–4), 208–213. https://doi.org/10.1111/j.1399-3011.1992.tb00293.x.

(26) Barany, G.; Merrifield, R. B. A New Amino Protecting Group Removable by Reduction. Chemistry of the Dithiasuccinoyl (Dts) Function. *J. Am. Chem. Soc.* **1977**, *99* (22), 7363–7365. https://doi.org/10.1021/ja00464a050.

(27) Chang, C. D.; Meienhofer, J. Solid-Phase Peptide Synthesis Using Mild Base Cleavage of N_{α}Fluorenylmethyloxycarbonylamino Acids, Exemplified By a Synthesis of Dihydrosomatostatin. *Int. J. Pept. Protein Res.* **1978**, *11* (3), 246–249. https://doi.org/10.1111/j.1399-3011.1978.tb02845.x.

(28) El-faham, A.; Albericio, F. Peptide Coupling Reagents, More than a Letter Soup. *Chem. Rev.* **2011**, 6557–6602. https://doi.org/10.1021/cr100048w.

(29) Pires, D. A. T.; Bemquerer, M. P.; Do Nascimento, C. J. Some Mechanistic Aspects on Fmoc Solid Phase Peptide Synthesis. *Int. J. Pept. Res. Ther.* **2014**, *20* (1), 53–69. https://doi.org/10.1007/s10989-013-9366-8.

(30) Zinieris, N.; Leondiadis, L.; Ferderigos, N. Nα-Fmoc Removal from Resin-Bound Amino Acids by 5% Piperidine Solution. *J. Comb. Chem.* **2005**, *7* (1), 4–6. https://doi.org/10.1021/cc049872d.

(31) Hachmann, J.; Lebl, M. Alternative to Piperidine in Fmoc Solid-Phase Synthesis. *J. Comb. Chem.* **2006**, *8* (2), 149. https://doi.org/10.1021/cc050123l.

(32) Ralhan, K.; KrishnaKumar, V. G.; Gupta, S. Piperazine and DBU: A Safer Alternative for

Rapid and Efficient Fmoc Deprotection in Solid Phase Peptide Synthesis. *RSC Adv.* **2015**, *5* (126), 104417–104425. https://doi.org/10.1039/c5ra23441g

(33) Jacobson, B. S.; Fairman, K. R. A Colorimetric Assay for Carbodiimides Commonly Used in Peptide Synthesis and Carboxyl Group Modification. *Anal. Biochem.* **1980**, *106* (1), 114–117. https://doi.org/10.1016/0003-2697(80)90125-6

(34) Merrifield, R. B. Solid State Synthesis (Nobel Lecture). *Angew. Chemie Int. Ed. Engl* **1985**, *24* (10), 799–810. https://doi.org/https://doi.org/10.1002/anie.198507993.

(35) Palomo, J. M. Solid-Phase Peptide Synthesis: An Overview Focused on the Preparation of Biologically Relevant Peptides. *RSC Adv.* **2014**, *4* (62), 32658–32672. https://doi.org/10.1039/c4ra02458c.

(36) Coste, J.; Le-Nguyen, D.; Castro, B. PyBOP®: A New Peptide Coupling Reagent Devoid of Toxic By-Product. *Tetrahedron Lett.* **1990**, *31* (2), 205–208. https://doi.org/10.1016/S0040-4039(00)94371-5

(37) Dourtoglou, V.; Ziegler, J. C.; Gross, B. L'hexafluorophosphate de O-Benzotriazolyl-*N*,*N*-Tetramethyluronium: Un Reactif de Couplage Peptidique Nouveau et Efficace. *Tetrahedron Lett.* **1978**, *19* (15), 1269–1272. https://doi.org/10.1016/0040-4039(78)80103-8

(38) Pedersen, S. L.; Tofteng, A. P.; Malik, L.; Jensen, K. J. Microwave Heating in Solid-Phase Peptide Synthesis. *Chem. Soc. Rev.* **2012**, *41* (5), 1826–1844. https://doi.org/10.1039/c1cs15214a.

(39) King, D. S.; Fields, C. G.; Fields, G. B. A Cleavage Method Which Minimizes Side Reactions Following Fmoc Solid Phase Peptide Synthesis. *Int. J. Pept. Protein Res.* **1990**, *36* (3), 255–266. https://doi.org/10.1111/j.1399-3011.1990.tb00976.x.

(40) Mehta, A.; Jaouhari, R.; Benson, T. J.; Douglas, K. T. Improved Efficiency and Selectivity in Peptide Synthesis: Use of Triethylsilane as a Carbocation Scavenger in Deprotection of *t*-Butyl Esters and *t*-Butoxycarbonyl-Protected Sites. *Tetrahedron Lett.* **1992**, *33* (37), 5441–5444. https://doi.org/10.1016/S0040-4039(00)79116-7

(41) Reeve, E. *Arabidopsis*. *Genet. Res.* **1995**, *66* (2), 180–181. https://doi.org/10.1017/s0016672300034546.

(42) Meinke, D. W.; Cherry, J. M.; Dean, C.; Rounsley, S. D.; Koornneef, M. *Arabidopsis Thaliana:* A Model Plant for Genome Analysis. *Science.* **1998**, *282* (5389), 662–682. https://doi.org/10.1126/science.282.5389.662.

(43) Eddy, R.; Hahn, D. T. Purdue Methods for *Arabidopsis* Growth: 101 Ways to Try to Grow *Arabidopsis*: What Soil Mix Worked the Best in This Study? *Purdue Methods Arabidopsis Growth* **2012**, Paper 2. https://docs.lib.purdue.edu/cgi/viewcontent.cgi?article=1001&context=pmag.

(44) Bennett, M. D.; Leitch, I. J.; Price, H. J.; Johnston, J. S. Comparisons with *Caenorhabditis* (~100 Mb) and *Drosophila* (~175 Mb) Using Flow Cytometry Show Genome Size in Arabidopsis to be ~157 Mb and Thus ~25% Larger than the Arabidopsis Genome Initiative Estimate of ~125 Mb. *Ann. Bot.* **2003**, *91* (5), 547–557. https://doi.org/10.1093/aob/mcg057.

(45) Clough, S. J.; Bent, A. F. Floral Dip: A Simplified Method for *Agrobacterium*-Mediated Transformation of *Arabidopsis Thaliana*. *Plant J.* **1998**, *16* (6), 735–743. https://doi.org/10.1046/j.1365-313X.1998.00343.x.

(46) Meyerowitz, E. M. Prehistory and History of Arabidopsis Research. *Plant Physiol.* **2001**, *125* (1), 15–19. https://doi.org/10.1104/pp.125.1.15.

(47) Meinke, D.; Scholl, R. Editor ' s Choice Series on Sharing Data and Materials The Preservation of Plant Genetic Resources. Experiences with *Arabidopsis* 1. *Plant Physiol.* **2003**, 133(3), 1046–50. https://doi.org/10.1104/pp.103.024877

(48) Alvarez-Buylla, E. R.; Benítez, M.; Corvera-Poiré, A.; Chaos Cador, Á.; de Folter, S.; Gamboa de Buen, A.; Garay-Arroyo, A.; García-Ponce, B.; Jaimes-Miranda, F.; Pérez-Ruiz, R. V.; Piñeyro-Nelson, A.; Sánchez-Corrales, Y. E. Flower Development. *The Arabidopsis Book.* **2010**, *8*, e0127. https://doi.org/10.1199/tab.0127.

(49) Irish, V. The ABC Model of Floral Development. *Curr. Biol.* **2017**, *27* (17), R887–R890. https://doi.org/10.1016/j.cub.2017.03.045.

(50) Chang, C.; Meyerowitz, E. M. Molecular Cloning and DNA Sequence of the *Arabidopsis Thaliana* Alcohol Dehydrogenase Gene. *Proc. Natl. Acad. Sci. U. S. A.* **1986**, *83* (5), 1408–1412. https://doi.org/10.1073/pnas.83.5.1408.

(51) Pierce, M.; Yu, D.; Richards-Kortum, R. High-Resolution Fiber-Optic Microendoscopy for in Situ Cellular Imaging. *J. Vis. Exp.* **2010**, No. 47, 6–10. https://doi.org/10.3791/2306.

(52) Krstajić, N.; Akram, A. R.; Choudhary, T. R.; McDonald, N.; Tanner, M. G.; Pedretti, E.; Dalgarno, P. A.; Scholefield, E.; Girkin, J. M.; Moore, A.; Bradley, M.; Dhaliwal, K. Two-Color Widefield Fluorescence Microendoscopy Enables Multiplexed Molecular Imaging in the Alveolar Space of Human Lung Tissue. *J. Biomed. Opt.* **2016**, *21* (04), 1. https://doi.org/10.1117/1.jbo.21.4.046009.

(53) Blanco-Canosa, J. B.; Dawson, P. E. An Efficient Fmoc-SPPS Approach for the Generation of Thioester Peptide Precursors for Use in Native Chemical Ligation. *Angew. Chem., Int. Ed.* **2008**, *47* (36), 6851–6855. https://doi.org/10.1002/anie.200705471.

(54) Zipfel, C.; Robatzek, S.; Navarro, L.; Oakeley, E. J.; Jones, J. D. G.; Felix, G.; Boller, T.

Bacterial Disease Resistance in Arabidopsis through Flagellin Perception. *Nature* **2004**, *428* (6984), 764–767. https://doi.org/10.1038/nature02485.

(55) Davern, S. M.; McKnight, T. E.; Standaert, R. F.; Morrell-Falvey, J. L.; Shpak, E. D.; Kalluri, U. C.; Jelenska, J.; Greenberg, J. T.; Mirzadeh, S. Carbon Nanofiber Arrays: A Novel Tool for Microdelivery of Biomolecules to Plants. *PLoS One* **2016**, *11* (4), 1–25. https://doi.org/10.1371/journal.pone.0153621.

(56) http://elifesciences.org/digests/43487/propelling

VITA

EDWARD OFFEI

Education:	M.S. Chemistry, East Tennessee State University, Johnson City, Tennessee, 2021
	BSc. Chemistry, Kwame Nkrumah University of Science and Technology, Kumasi, Ashanti Region, 2016
Professional Experience:	Graduate Teaching Assistant, East Tennessee State University, College of Arts and Sciences, 2019–2021
	Research and Administrative Assistant, University of Ghana, College of Basic and Applied Sciences, 2016-2018